



Calhoun: The NPS Institutional Archive
DSpace Repository

Theses and Dissertations

1. Thesis and Dissertation Collection, all items

2008-06

High-speed blade vibration in a transonic compressor

Murphy, William P.

Monterey California. Naval Postgraduate School

<https://hdl.handle.net/10945/4052>

This publication is a work of the U.S. Government as defined in Title 17, United States Code, Section 101. Copyright protection is not available for this work in the United States.

Downloaded from NPS Archive: Calhoun



Calhoun is the Naval Postgraduate School's public access digital repository for research materials and institutional publications created by the NPS community. Calhoun is named for Professor of Mathematics Guy K. Calhoun, NPS's first appointed -- and published -- scholarly author.

Dudley Knox Library / Naval Postgraduate School
411 Dyer Road / 1 University Circle
Monterey, California USA 93943

<http://www.nps.edu/library>



NAVAL POSTGRADUATE SCHOOL

MONTEREY, CALIFORNIA

THESIS

**HIGH-SPEED BLADE VIBRATION IN A TRANSONIC
COMPRESSOR**

by

William P. Murphy

June 2008

Thesis Advisor:
Co-Advisor:

Garth V. Hobson
Steven Baker

Approved for public release; distribution is unlimited.

THIS PAGE INTENTIONALLY LEFT BLANK

REPORT DOCUMENTATION PAGE			Form Approved OMB No. 0704-0188
Public reporting burden for this collection of information is estimated to average 1 hour per response, including the time for reviewing instruction, searching existing data sources, gathering and maintaining the data needed, and completing and reviewing the collection of information. Send comments regarding this burden estimate or any other aspect of this collection of information, including suggestions for reducing this burden, to Washington headquarters Services, Directorate for Information Operations and Reports, 1215 Jefferson Davis Highway, Suite 1204, Arlington, VA 22202-4302, and to the Office of Management and Budget, Paperwork Reduction Project (0704-0188) Washington DC 20503.			
1. AGENCY USE ONLY (Leave blank)	2. REPORT DATE June 2008	3. REPORT TYPE AND DATES COVERED Master's Thesis	
4. TITLE AND SUBTITLE High-Speed Blade Vibration in a Transonic Compressor		5. FUNDING NUMBERS	
6. AUTHOR(S) William P. Murphy		8. PERFORMING ORGANIZATION REPORT NUMBER	
7. PERFORMING ORGANIZATION NAME(S) AND ADDRESS(ES) Naval Postgraduate School Monterey, CA 93943-5000		10. SPONSORING/MONITORING AGENCY REPORT NUMBER	
9. SPONSORING /MONITORING AGENCY NAME(S) AND ADDRESS(ES) N/A		11. SUPPLEMENTARY NOTES The views expressed in this thesis are those of the author and do not reflect the official policy or position of the Department of Defense or the U.S. Government.	
12a. DISTRIBUTION / AVAILABILITY STATEMENT Approved for public release; distribution is unlimited.		12b. DISTRIBUTION CODE	
13. ABSTRACT (maximum 200 words) This experiment was conducted to measure transverse vibrations of the blades in a transonic compressor rig at the Naval Postgraduate School. The compressor was instrumented with non-invasive laser light probes to measure changes in time of arrival of all the blades, relative to an expected arrival time. These times were then converted to blade deflections. Results proved that the primary observed vibration was a first bending mode. The frequencies that excited this mode precisely correlated with NASA predictions. It was shown that the modal frequency for the first bending mode was dependent on engine speed as a result of the untwisting blade. Maximum observed blade deflection was proved to occur during the surge event, resulting in maximum blade fatigue. It was concluded that certain operating regimes, with large blade deflections, should be avoided to extend blade life by limiting fatigue.			
14. SUBJECT TERMS Compressor, Transonic, NSMS, Laser Light Probes, Stall, Campbell Diagram, Bending Modes, Vibration.		15. NUMBER OF PAGES 57	
		16. PRICE CODE	
17. SECURITY CLASSIFICATION OF REPORT Unclassified	18. SECURITY CLASSIFICATION OF THIS PAGE Unclassified	19. SECURITY CLASSIFICATION OF ABSTRACT Unclassified	20. LIMITATION OF ABSTRACT UU

NSN 7540-01-280-5500

Standard Form 298 (Rev. 2-89)
Prescribed by ANSI Std. Z39-18

THIS PAGE INTENTIONALLY LEFT BLANK

Approved for public release; distribution is unlimited.

HIGH-SPEED BLADE VIBRATION IN A TRANSONIC COMPRESSOR

William P. Murphy
Ensign, United States Navy
B.S., United States Naval Academy, 2007

Submitted in partial fulfillment of the
requirements for the degree of

MASTER OF SCIENCE IN ENGINEERING ACOUSTICS

from the

**NAVAL POSTGRADUATE SCHOOL
June, 2008**

Author: William P. Murphy

Approved by: Garth V. Hobson
Thesis Advisor

Steven Baker
Co-Advisor

Kevin B. Smith
Chairman, Engineering Acoustics Academic Committee

THIS PAGE INTENTIONALLY LEFT BLANK

ABSTRACT

This experiment was conducted to measure transverse vibrations of the blades in a transonic compressor rig at the Naval Postgraduate School. The compressor was instrumented with non-invasive laser light probes to measure changes in time of arrival of all the blades, relative to an expected arrival time. These times were then converted to blade deflections. Results proved that the primary observed vibration was a first bending mode. The frequencies that excited this mode precisely correlated with NASA predictions. It was shown that the modal frequency for the first bending mode was dependent on engine speed as a result of the untwisting blade. Maximum observed blade deflection was proved to occur during the surge event, resulting in maximum blade fatigue. It was concluded that certain operating regimes, with large blade deflections, should be avoided to extend blade life by limiting fatigue.

THIS PAGE INTENTIONALLY LEFT BLANK

TABLE OF CONTENTS

I.	INTRODUCTION.....	1
II.	EXPERIMENTAL APPARATUS AND PROCEDURE DESCRIPTION.....	5
	A. TEST EQUIPMENT.....	5
	B. APPROACH TO THE TESTING PROCESS.....	9
	C. METHOD OF DATA ACQUISITION.....	11
	D. TESTING PROCEDURE.....	12
III.	ANALYTICAL PROCEDURE.....	15
	A. MODEL DEVELOPMENT.....	15
IV.	RESULTS.....	17
	A. MODAL RESULTS.....	17
	B. SANGER ROTOR CAMPBELL DIAGRAM ANALYSIS.....	20
	C. DEVELOPMENT OF FIRST BENDING MODE ASSUMPTION.....	21
	D. EXPERIMENTAL CAMPBELL DIAGRAM DEVELOPMENT.....	24
	E. THEORETICAL TO EXPERIMENTAL COMPARISON.....	28
V.	CONCLUSIONS AND RECOMMENDATIONS.....	31
	LIST OF REFERENCES.....	33
	APPENDIX: SOFTWARE INSTRUCTIONS.....	35
	INITIAL DISTRIBUTION LIST.....	41

THIS PAGE INTENTIONALLY LEFT BLANK

LIST OF FIGURES

Figure 1.	Total system schematic of the transonic compressor rig.....	5
Figure 2.	The transonic compressor rig at the Naval Postgraduate School.....	6
Figure 3.	Mounting bolt and laser light probe with fiber optic cable	7
Figure 4.	Laser power supply and receiving optics.....	8
Figure 5.	Two blade vibration sensor interface boards (BVSI).....	9
Figure 6.	Longitudinal view of the system casing from the rear of the system...	11
Figure 7.	Screenshot of software record function	13
Figure 8.	Screenshot of data for 95% speed, open throttle setting.....	13
Figure 9.	Connected blade profiles.....	15
Figure 10.	Tetrahedron mesh of the blade volume	16
Figure 11.	First bending mode of the blade	17
Figure 12.	First torsion mode of the blade	18
Figure 13.	Second bending mode of the blade	18
Figure 14.	First edgewise bending mode of the blade	19
Figure 15.	Second torsion mode of the blade	19
Figure 16.	Sanger rotor Campbell diagram	20
Figure 17.	RPM trace of 90% speed stall	21
Figure 18.	Compressor performance map.....	22
Figure 19.	Raw timing data from 90% data test.....	22
Figure 20.	Expanded raw timing data	23
Figure 21.	Waterfall plot	24
Figure 22.	Nodal diameter description.....	25
Figure 23.	Campbell diagram single data set	26
Figure 24.	Campbell diagram all data.....	27
Figure 25.	Campbell diagram side by side comparison	28

THIS PAGE INTENTIONALLY LEFT BLANK

LIST OF TABLES

Table 1.	Material Properties AL7075-T6 [From 6]	6
Table 2.	Sanger stage parameters [From 8].....	7
Table 3.	Inputted data into blade pass software for 80 MHz	11
Table 4.	Modal frequencies	17
Table 5.	Campbell diagram comparison	29

THIS PAGE INTENTIONALLY LEFT BLANK

ACKNOWLEDGMENTS

I would like to thank the staff at the Naval Postgraduate School Turbopropulsion Lab. Specifically, I would like to thank Dr. Garth Hobson, Dr. Anthony Gannon, and Mr. Doug Seivwright for answering every question that I could possibly ask related to turbomachinery. Also, I would like to thank Mr. John Gibson for always fixing any problem that I encountered during this project. To Mr. Peter Tappert and Hood Technologies a thank you, for much needed technical assistance using the BVSI software. Finally, thank you to my family and friends for keeping me on a track to finish this thesis.

THIS PAGE INTENTIONALLY LEFT BLANK

I. INTRODUCTION

High-speed turbomachinery such as the transonic test compressor at the Naval Postgraduate School can experience tremendous centrifugal and gas bending loads. High-speed operation for such a system is commonplace. As a result, the compressor blades must be able to withstand high frequency oscillations of such loads due to either stall and surge, or rotor-stator interactions. Prior to this experiment there was no instrumentation in place to monitor the displacement of the blades during operation of the system. Such instrumentation provided valuable data on expected blade life of the system and on anticipated blade vibrations at specific engine speeds.

The use of laser light probes to monitor blade vibration is not a new method of data acquisition. Historically, the use of strain gauges, internally mounted pressure transducers, and laser light probes have provided the methods for measuring blade vibration in high-speed turbomachinery. Laser light probes have the advantage of being non-invasive. They can provide accurate results without altering the characteristics of the blade. Strain gauges, while relatively inexpensive, present the challenge of being externally adhered to the blades, while internally mounted pressure transducers only respond to the normal pressure fluctuations on the blade surface. The pressure transducers are also expensive, and are further limited by altering the internal geometry of the blade, resulting in different modal frequencies. Both strain gauges and internally mounted pressure transducers encounter problems in capturing the data from the blade and moving it to an external data acquisition system in real time. The solution to this problem is the use of a slip ring, which is both costly and complicated.

The major limitation of laser light probes is the inability to gain information on higher order modes of vibration. Each probe can only take data at a specific location along the arc of the blade, as well as at specific locations circumferentially around the casing. Blade displacement due to vibration could

occur where no laser probes are located, and the vibration would not be experimentally observed. Strain gauges and internal pressure transducers can record vibrations continuously as the blades rotate around the shaft. However, such sensors can be limited if mounted on or near a node (a point of zero displacement) or anti-node of the system.

Since the modes that could be easily excited and resolved in this analysis were lower order (i.e. first through third), laser light probes were a good choice. This choice was justified because, when lower order modes are excited in a fixed-free bar, maximum displacement occurs at an anti-node. By definition of the system's boundary conditions, one such anti-node occurs at the free end of the bar, closest to the casing. Since the laser light probes were mounted within the casing (and it was assumed that the blade would undergo similar displacements to that of a straight bar), they were in very close proximity to the point of maximum displacement. This made laser light probes a desirable system to resolve blade vibration in this configuration.

Prior research in the study of blade vibration using laser light probes has been conducted at NPS by Osburn [2]. Osburn was able to validate the time of arrival (TOA) data obtained by the laser light probes using strobe photography and thus justify that such probes were able to resolve accurate speed and timing data.

The problem of stall side flutter was addressed in 2003 by Sanders, Rabe and Hassen [3]. They examined blade displacement due to the first torsion (primary) and first bending modes. The fan blisk was a twenty-two bladed transonic system (similar to the TCR) and employed both strain gauges and miniature pressure transducers to monitor blade vibration as a response to flutter.

Each blade is in essence a bar, fixed spatially at one end and free at the other. As a result, from the solution of the transverse wave equation, natural frequencies for the lower order modes of a bar were developed for comparison [1]. Since the geometry of the blade was not that of a simple bar, a finite element

analysis was performed on the blade shape to predict the modal frequencies, and in turn predict engine speeds at which maximum blade displacement was likely to occur. These relationships can be seen in the Campbell diagram of a specific system. The Campbell diagram for this system was verified for the first bending response during this experiment.

Laser light probes were mounted along the casing of the transonic compressor rig (TCR) at specific locations relative to the blades. This mounting position allowed the tip displacement of the blades to be measured. Measured tip displacement could then be correlated to specific engine speeds and modal frequencies to determine operating speeds that should be avoided to increase the structural life of the blades.

THIS PAGE INTENTIONALLY LEFT BLANK

II. EXPERIMENTAL APPARATUS AND PROCEDURE DESCRIPTION

A. TEST EQUIPMENT

The complete system that was used in this testing was a combination of non-intrusive sensors (laser light probes), high-speed pressure transducers, and hot-wire probes mounted on the transonic compressor rig. The schematic of all sensors employed in the system can be seen below.

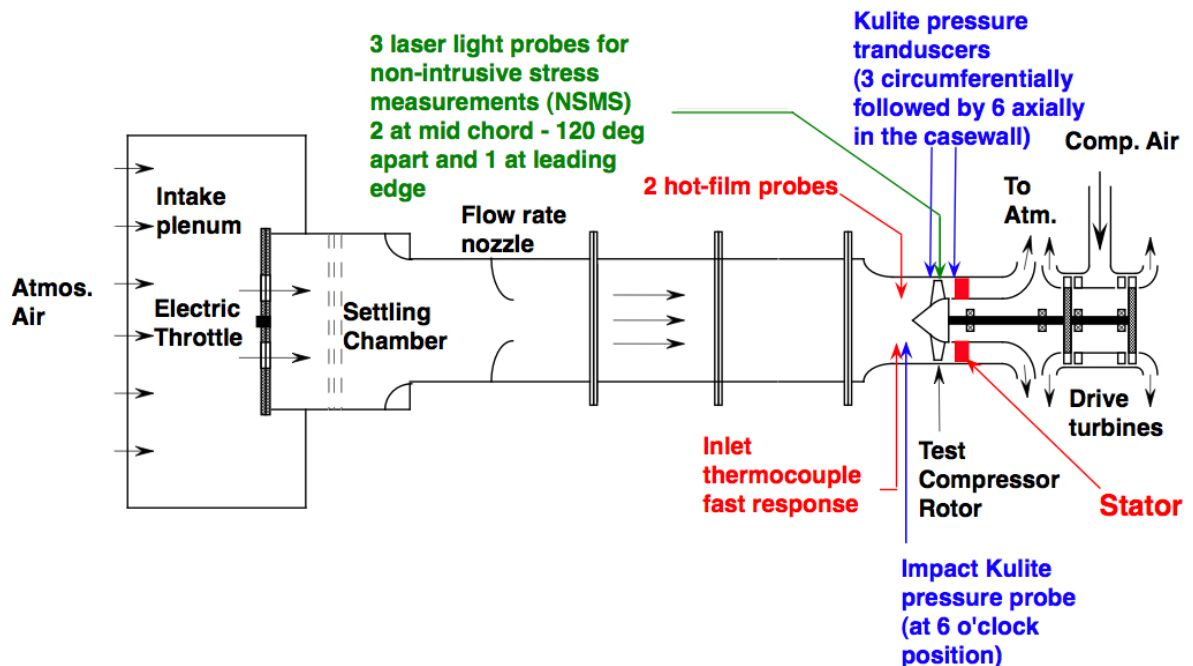


Figure 1. Total system schematic of the transonic compressor rig

This experimentation focused on the data taken from the non-intrusive stress measurement sensors (NSMS) shown above in green. The NSMS system consisted of three laser light probes configured around the casing of the transonic compressor rig. This NSMS experimentation was run in conjunction with other testing using both Kulite pressure transducers and hot-wire probes.

The transonic compressor rig (TCR) located in the Turbopropulsion Laboratory on the campus of the Naval Postgraduate School is shown in Figure 2. The TCR has a nominal pressure ratio of one and one-half. The compressor

was designed by NASA specifically for this rig using CFD techniques [8]. The light probe experimentation was done on the stage configuration of the TCR, with a 22 blade rotor and a 27 blade stator made of a high strength aluminum alloy, Al 7075-T6. The material properties of Al 7075-T6 are presented in Table 1. The drive turbines (Figure 2) were driven by an Allis-Charmers compressor which in turn drove the test compressor. Air was pulled from atmosphere through flow straighteners and into the compressor. The throttle, which dictated the mass flow into the system was electronically actuated. The Sanger Stage Parameters for the stage configuration can be seen in Table 2. For a more detailed description of the system see Zarro [7].



Figure 2. The transonic compressor rig at the Naval Postgraduate School

Table 1. Material Properties AL7075-T6 [From 6]

Attribute	Value	Units
Young's Modulus	71.75	GPa
Density	2740	kg/m ³
Poisson's Ratio	0.33	

Table 2. Sanger stage parameters [From 8]

Parameter	Value
Rotor Pressure Ratio	1.61
Stage Pressure Ratio	1.56
Tip Speed	396.2 m/s
Design Weight Flow	7.75 kg/s
Specific Weight Flow	170.9 kg/sec-m ²
Specific Head Rise	0.246
Tip Inlet Relative Mach Number	1.28
Aspect Ratio	1.2
Hub/Tip Radius Ratio	0.51
Number of Rotor Blades	22
Number of Stator Blades	27
Tip Solidity- Rotor	1.3
Tip Solidity- Stator	1.0
Outside Diameter	.2794 m
Rotor Diffusion Factor- Tip	0.4
Rotor Diffusion Factor- Hub	0.47
Stator Diffusion Factor- Tip	0.52
Stator Diffusion Factor- Hub	0.58

Laser light probes were used to measure the time of arrival of the blade tips during this experiment. Each probe consisted of a red, He-Ne, laser located concentrically to a circular receiver. This receiver detected the laser reflections off surfaces within a close proximity to the laser (approximately 2.0 cm). That signal was then transmitted via collection fiber optic cables to the receiver stand. For the test data sets, three of these probes were mounted around the casing of the TCR. They were used to measure the time difference between specific blade passes in order to determine blade deflection.



Figure 3. Mounting bolt and laser light probe with fiber optic cable

The laser transmitter and receiver stand was capable of managing signals from up to four laser probes simultaneously. The light that reflected off of the blade surface was received via the light probe and transmitted to the test stand. When the power of the received signal reached a defined level, a time stamped voltage, proportional to that power was sent to the acquisition computer via the Blade Vibration Sensor Interface (BVS) boards. The voltage level to trigger that signal was controlled by the BVS boards and could be manually altered depending on the strength of the reflected laser.

There were two BVS boards used. Each board acted as an interface between the test stand and the acquisition software for up to two probes and a once per revolution signal. The boards were essentially amplifiers that provided adjustable gain within the trigger levels. The paired boards could simultaneously manage signals from up to four probes, and control the trigger levels for each probe individually. The once per revolution (OPR) signal for each board had to be identical to the other. As a result, a single OPR signal was split between the two boards.

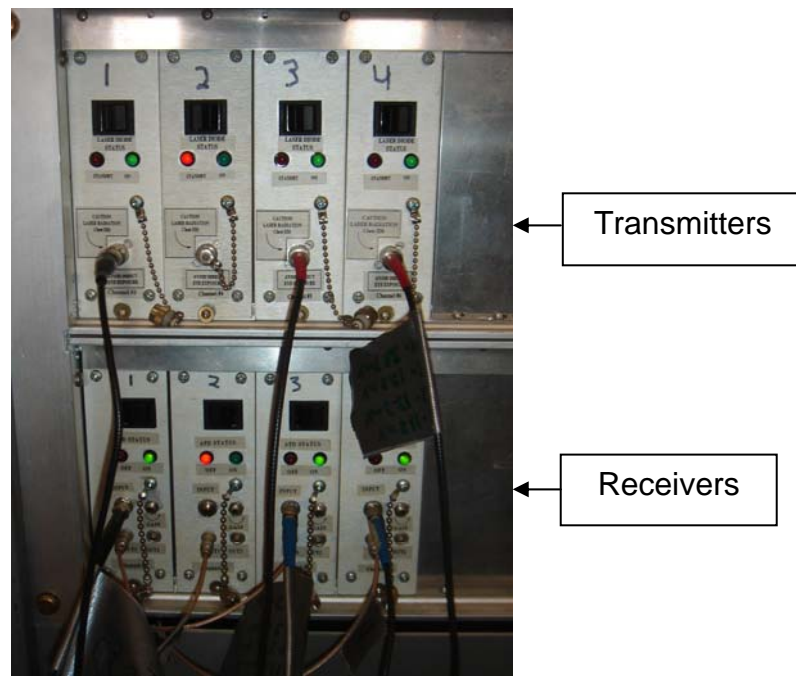


Figure 4. Laser power supply and receiving optics

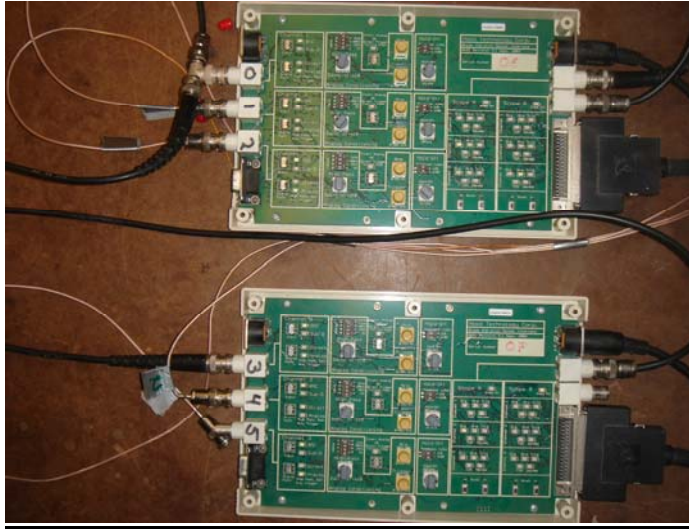


Figure 5. Two blade vibration sensor interface boards (BVSI)

The Blade Vibration Interface Software, which was used as the data acquisition software, was developed by Hood Technologies of Mt. Hood, Oregon [4]. The software received the data from each of the probes through the BVSI boards and used precise time measurements to record blade positions relative to an expected arrival time. The data required to initialize the program were: number and diameter of blades, and the location of the probes along the casing. Using this data the software was able to develop an extremely accurate anticipated arrival time for each blade passing each probe.

B. APPROACH TO THE TESTING PROCESS

Prior to the insertion of the laser light probes into the casing of the TCR there was no method for securing their depth. As a result, the plug bolts that were in place to block the test holes in the casing wall were used for this purpose. A hole with a diameter just larger than that of the probe was drilled through the plug bolts so that the probe (without the casing) could be snugly inserted into the hole. A smaller hole was then drilled perpendicular to the first hole through the head of the bolt. That hole was then tapped, and a locking

screw was inserted. The locking screw prevented the probe from slipping due to the vibration of the rig itself. The probes were then mounted flush with the inner wall of the casing of the TCR, which allowed the probes to be mounted within close proximity to the blades without potential for damage.

The probes themselves were then calibrated for the experiment. It was desirable to arrange the probes in such a way so as to maximize the laser power output from each, while achieving the maximum average outputted power from all the probes simultaneously. The outputted power from each probe proved to be a function of multiple variables. In order to test this, a laser power meter was used to measure the outputted power from each probe in every possible configuration. The probes were then numbered according to the corresponding station that maximized the average power.

In addition to the probes being calibrated, the software had to be configured. For this, two function generators were used to approximate the signals that would be inputted to the software by the BVS1 boards. Since there were twenty-two individual blades on the compressor, one function generator modeled an impulse signal corresponding to once per revolution while the other modeled twenty-two impulse signals in that same time period. This data was fed as real system data into the software. As a trial, that data was recorded and analyzed. Obviously, it yielded no meaningful results, but it did prove that the system was configured correctly.

In initial testing of the system, one of the probes was damaged, leaving only three laser probes for the actual testing. As a result, the probes had to be positioned in such a way as to maximize the information that could be ascertained from the data. This configuration can be seen in the following diagram.

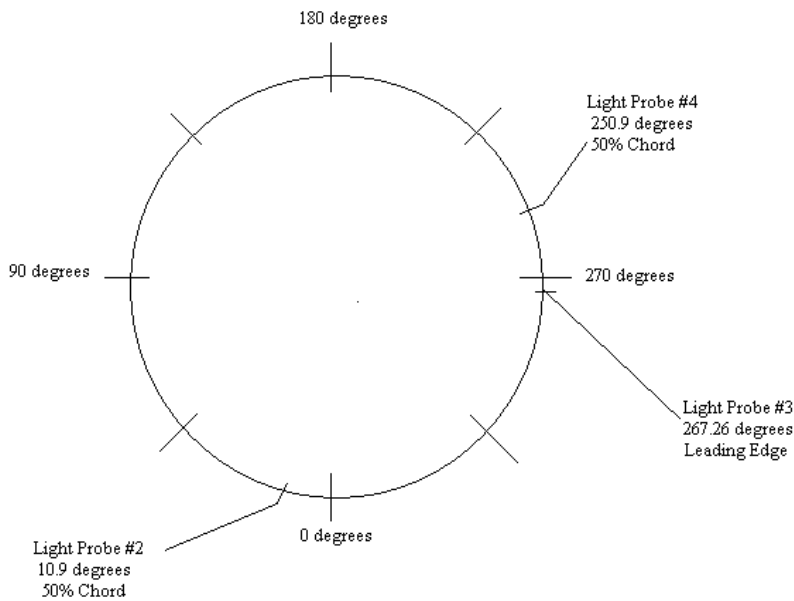


Figure 6. Longitudinal view of the system casing from the rear of the system

C. METHOD OF DATA ACQUISITION

As mentioned, the laser probes measured the passing of each blade by sensing the reflection of the emitted laser off of the metallic surface of that specific blade. The software used the inputted data seen in the table below to compute the time between multiple passes of a specific blade.

Table 3. Inputted data into blade pass software for 80 MHz

BVM Channel	Device	Label	Pulse Train Type	# Blades	Diameter (in)	Location (deg)
0	0	1/rev	TOA Only	1	11	0
1	0	Probe # 4	TOA Only	22	11	250.9
2	0	Probe # 3	TOA Only	22	11	267.3
3	1	1/rev	TOA Only	1	11	0
4	1	Probe # 2	TOA Only	22	11	10.9

As seen in the above table, the inputted data included: how to trigger the signal, the blade number, probe location, and diameter, as well how each probe was connected to the computer via the BVS1 boards.

From the inputted data, the software used the blade diameter, blade number, and probe location, as well as a measured rotor once-per-revolution (OPR) signal to compute a highly accurate prediction of arrival time. This prediction was made for all blades at each individual probe. As a result, the software was able to continuously predict a relative time when each blade should pass each probe. The laser light probe data was used in conjunction with an 80 MHz clock to record the specific time that each blade passed each probe. The software computed the time difference between the anticipated (non-vibrating) arrival time and the measured arrival time. Using the measured rotor speed with a known blade diameter, the software was able to correlate that time difference to a positive or negative blade deflection on the order of 0.025 mm (one thousandth of an inch). This calculation was performed for all blades for each revolution, with the engine operating at a nominal speed of 25,000 RPM.

D. TESTING PROCEDURE

Each individual test correlated to a specific percentage of the maximum rotational speed of the compressor. The data collected for this experimentation included 80, 90, and 95 percent of the maximum compressor speed (27,085 RPM). Each of those data sets was taken separately. Once a percentage of the compressor speed was chosen for the specific test, the TCR was run through start up procedures. The first data set taken was at steady state with open throttle. To obtain the data, the Acquire and then Record functions of the blade pass software were employed. Data was then taken for each subsequent throttle setting at that engine speed. When the system neared stall, both steady state and unsteady data were taken. The unsteady data was observed as the throttle setting changed, and the steady state data as taken after the compressor's speed stabilized. Unsteady data was also taken for steam ingestion tests, in which steam was injected into the system upstream of the compressor.

The blade pass software was used to capture these data sets and was recorded graphically as seen in the figures below.

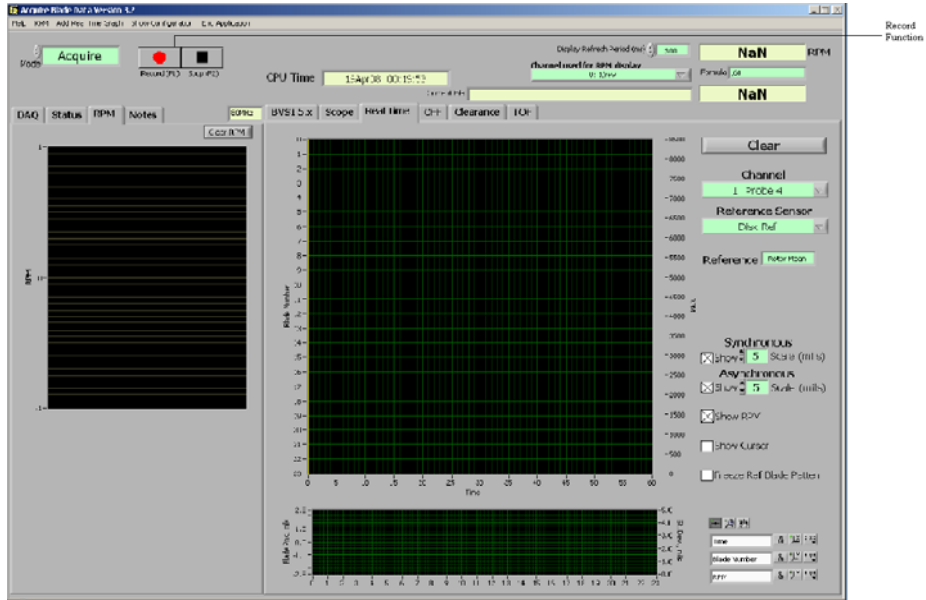


Figure 7. Screenshot of software record function

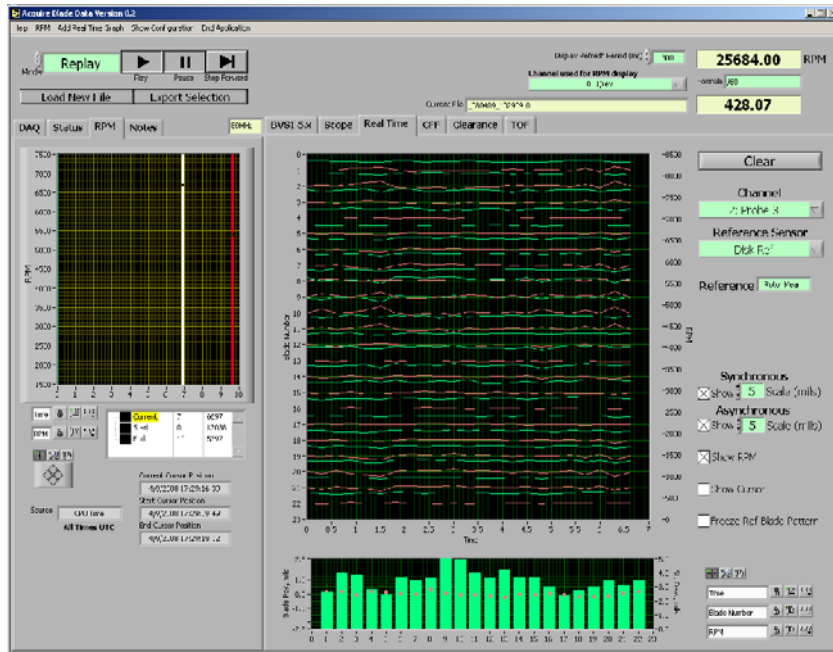


Figure 8. Screenshot of data for 95% speed, open throttle setting

THIS PAGE INTENTIONALLY LEFT BLANK

III. ANALYTICAL PROCEDURE

A. MODEL DEVELOPMENT

In order to develop the five frequencies corresponding to the first five modes of vibration, ANSYS software was used to construct a finite element model. This model employed thirty points in space which corresponded to the physical blade geometry. These points were separated into three planes where the planes corresponded to the hub, middle, and tip of the blade profile respectively. The profiles were connected in the span-wise axis of the blade as seen in Figure 9. Three areas of these profiles were then created, and then a single volume defined by those areas was developed. The volume was then fixed in space along the compressor hub to satisfy the system boundary conditions. The geometry was then meshed using a tetrahedron mesh to avoid ambiguity along the leading edge area, as seen in Figure 10. A modal analysis was then completed with 529 nodes and 222 elements. The modal analysis yielded the eigenvalues of the stiffness matrix and in turn was used to develop the modal shapes or vibration modes.

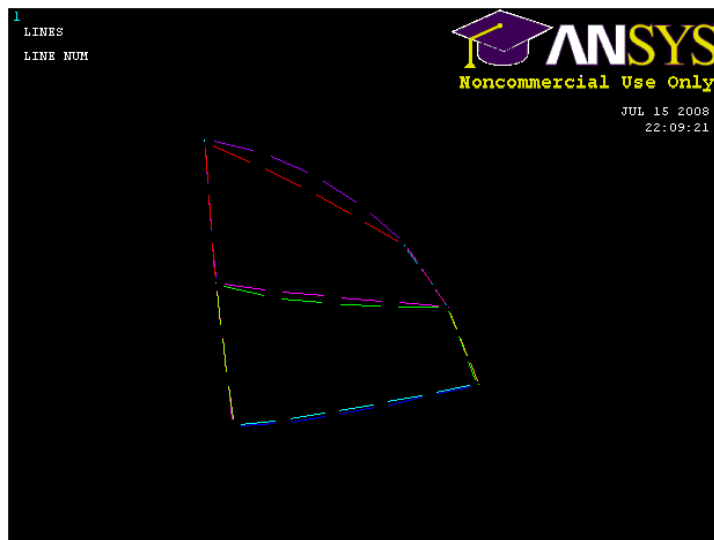


Figure 9. Connected blade profiles

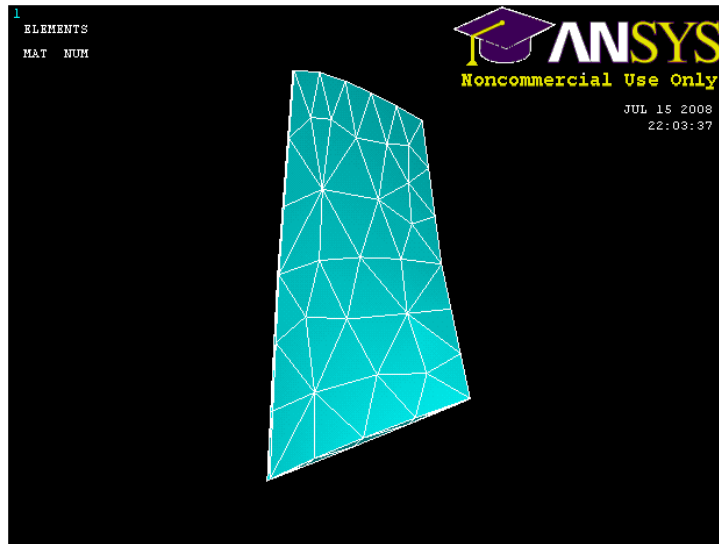


Figure 10. Tetrahedron mesh of the blade volume

IV. RESULTS

A. MODAL RESULTS

The meshed compressor blade that was spatially fixed at the hub yielded the following frequencies (seen in Table 4) for the first five modes of vibration. The first three modes compared favorably to those predicted by NASA [8] during the design of the rotor by Sanger.

Table 4. Modal frequencies

Mode	Frequency (Hz)	NASA Predictions (Hz)
1	755.81	750
2	2,659.60	2,700
3	2,786	3,050
4	4,758.40	
5	5,670.10	

The analysis of the blade yielded the relative displacements shown below. The displacements for the first bending mode are seen in Figure 11.

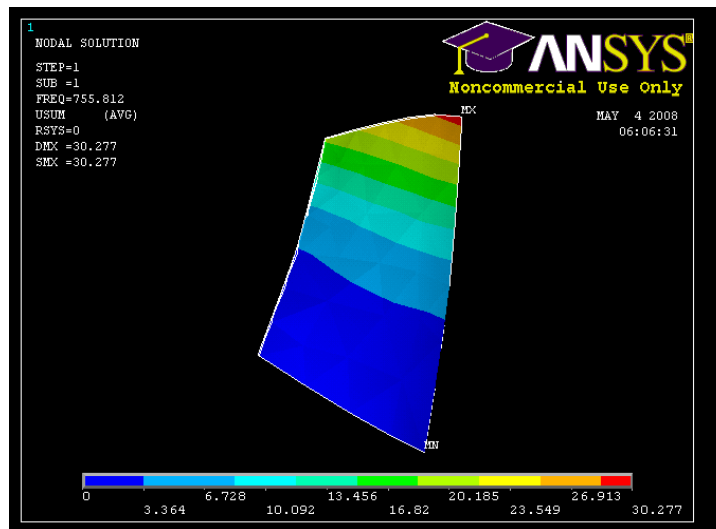


Figure 11. First bending mode of the blade

The presented frequency for the first bending mode, 755.81 (Hz) closely matched the first bending mode presented in the Campbell diagram shown in the

next section. The curve presented in that figure accounts for the untwisting of the blade with increasing engine speed. The first bending mode curve presented on the Campbell diagram below is based on empirical predictions by NASA accounting for the untwisting blade. The ANSYS finite element model did not account for this but proved to be a very good baseline, low engine speed estimate. The second through fifth vibration modes are presented in figures 12 through 15 respectively. The second mode (Figure 12) is representative of the first torsion mode of the blade, with differing deflections along the chord of the blade. The third mode (Figure 13) corresponds to the second bending mode of the blade. Figure 14, which is the fourth mode, shows an edgewise bending mode. The fifth mode presented as Figure 15 shows a higher order torsion mode.

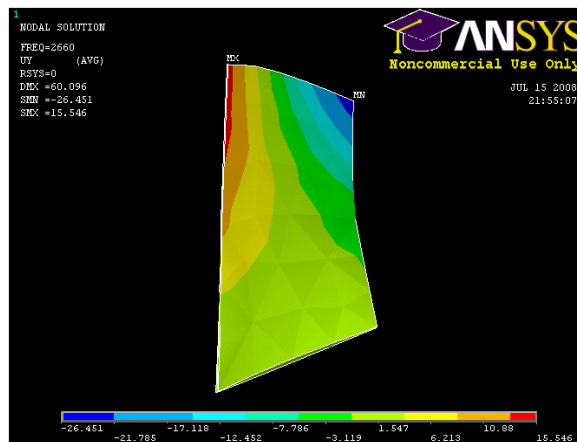


Figure 12. First torsion mode of the blade

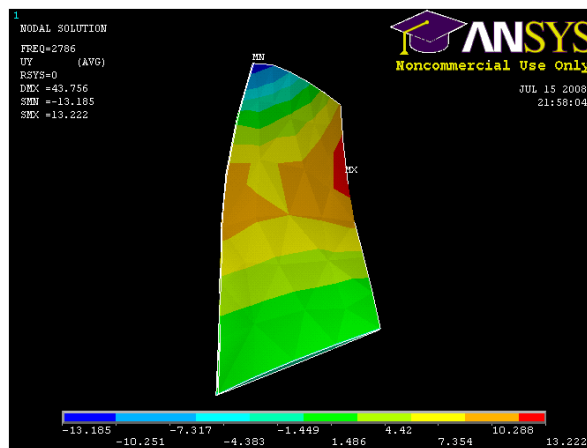


Figure 13. Second bending mode of the blade

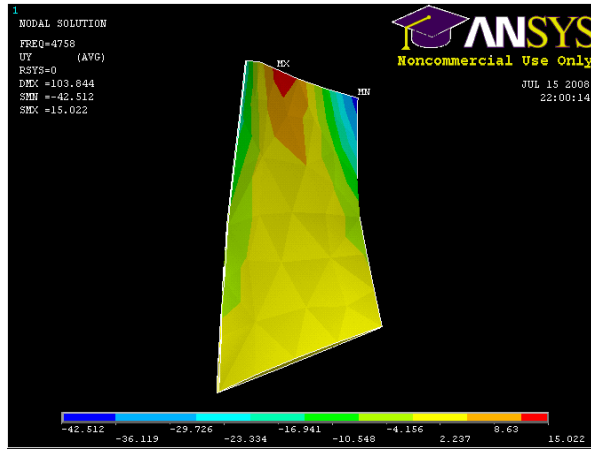


Figure 14. First edgewise bending mode of the blade

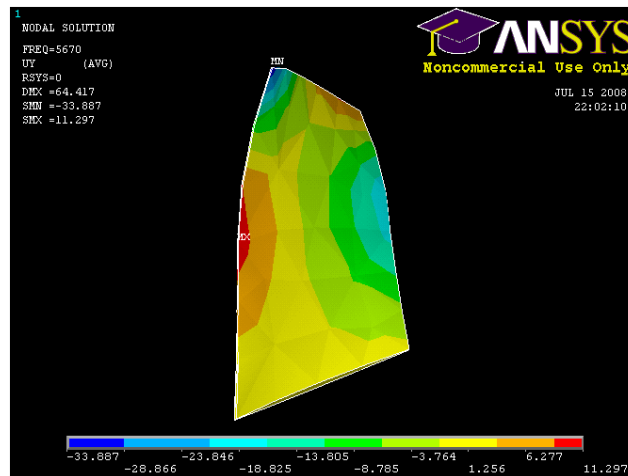


Figure 15. Second torsion mode of the blade

B. SANGER ROTOR CAMPBELL DIAGRAM ANALYSIS

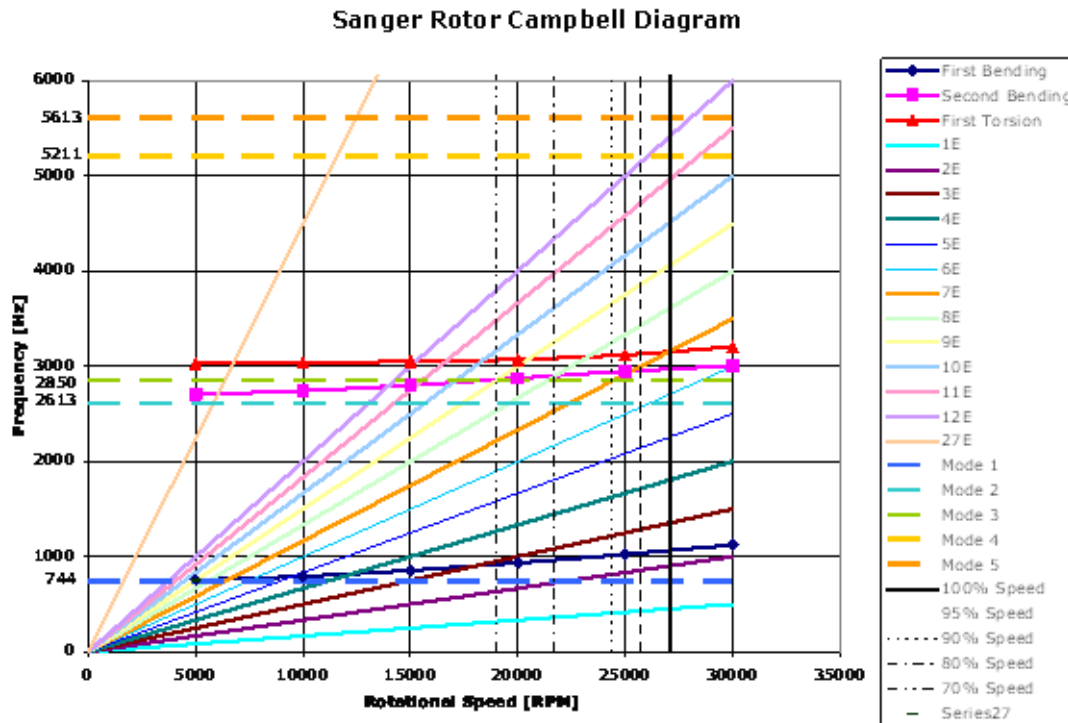


Figure 16. Sanger rotor Campbell diagram

The Sanger diagram above depicts engine rotational speed in RPM on the abscissa and frequency of vibration in Hertz on the ordinate. It shows plots of both engine orders and bending and torsion modes. The dotted lines corresponding to the modes are extensions of the low speed ANSYS predictions, while the solid lines are NASA predications from empirical data. Engine order is represented by the solid lines stemming from the origin and can be best described as the number of transverse vibrations a blade undergoes per revolution. For example, an engine order of one means that a given blade will oscillate through one cycle as it rotates one full revolution. Above it can be seen that at an engine speed of 30,000 RPM, the first engine order is at 500 Hz. Also from the diagram it can be seen that the first bending mode at 30,000 RPM should occur at approximately 1,100 Hz. The difference between the 1,100 Hz depicted in the Campbell diagram and the ANSYS modal solution that yielded 755.81 Hz is again, due to the untwisting of the blade with increasing speed.

From this diagram areas of interest can also be observed. Fatigue on a blade can be related to both frequency of vibration and the magnitude of the corresponding deflection. Since deflection magnitude drops significantly with higher order bending modes, some of the least optimal running conditions in terms of blade fatigue can occur at lower order bending modes (large deflection) and high engine orders (frequent deflection). One such operating area presented in the Campbell diagram is easily achievable by the TCR. That area of operation can be seen to be the intersection of the third engine order and the first bending mode. This would result in three large transverse deflections per revolution at an engine speed of approximately 18,000 RPM.

C. DEVELOPMENT OF FIRST BENDING MODE ASSUMPTION

For simplicity the figures from one data set will be shown for the following development. All figures correspond to the steam stall test conducted at 90 percent speed or 24,375 RPM. That test yielded the RPM trace shown below and analysis was conducted on probes three and four.

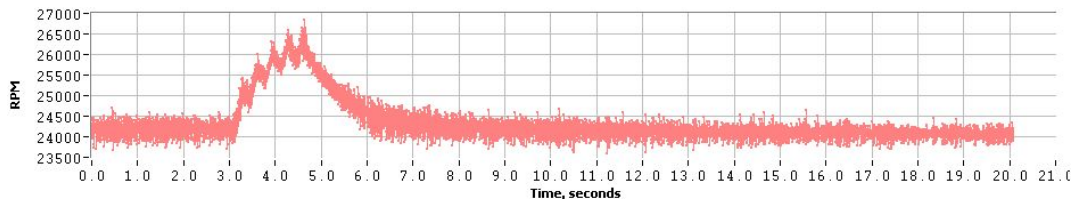


Figure 17. RPM trace of 90% speed stall

The area of interest can be seen in the above RPM trace between 2.0 and 7.0 seconds. This time period corresponded to the surge event shown, which resulted from steam injection at a throttle setting of 7.4. This operating area can be seen as the intersection of the curves corresponding to steam surge and 90 percent speed data, point A presented in Figure 18. These data correspond to the transient response of the injection of a slug of steam. During the steam injection, the compressor was forced into a surge cycle which can be seen in the RPM trace presented as Figure 17.

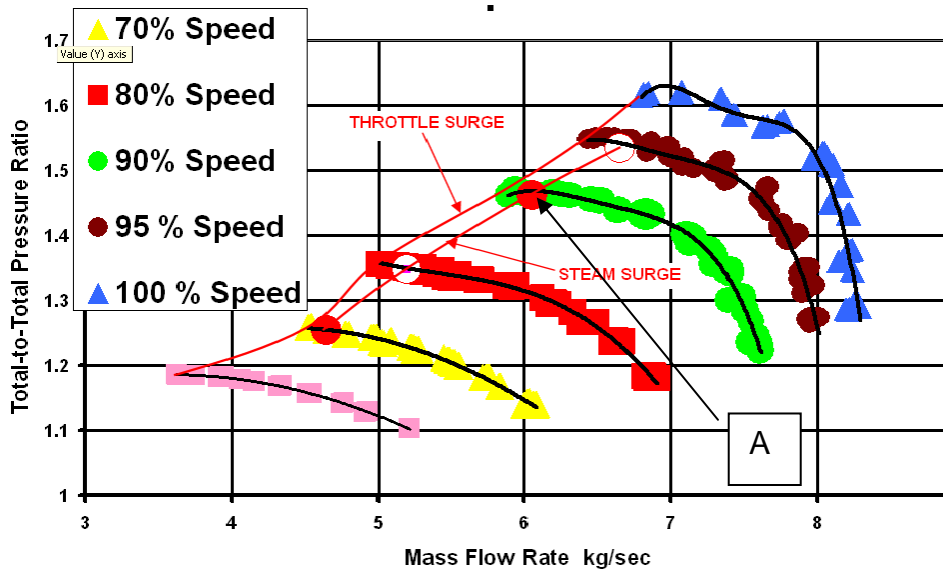


Figure 18. Compressor performance map

From the synchronous timing data extracted from the laser light probes, specifically from probes three and four, the assumption can be made that the primary response of the blades was in the first bending mode. The raw timing data can be extracted as shown below.

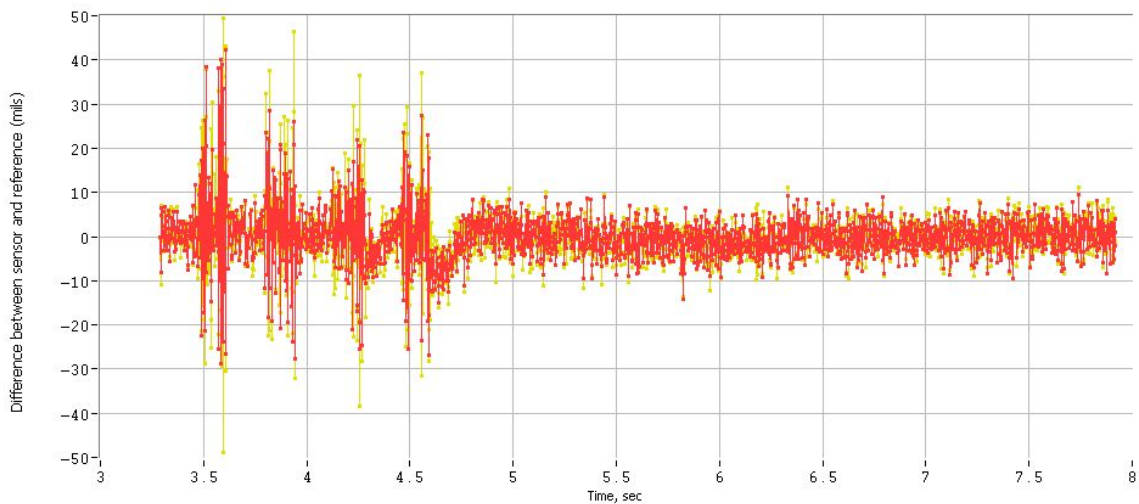


Figure 19. Raw timing data from 90% data test

It can be seen in the above diagram that greatest blade displacement from the reference occurs at times that corresponded to the surge event. Specifically, it appears that for each of the saw tooth spikes in RPM there is a corresponding maximum in blade displacement. Zooming in on the first spike in displacement yields the following plot.

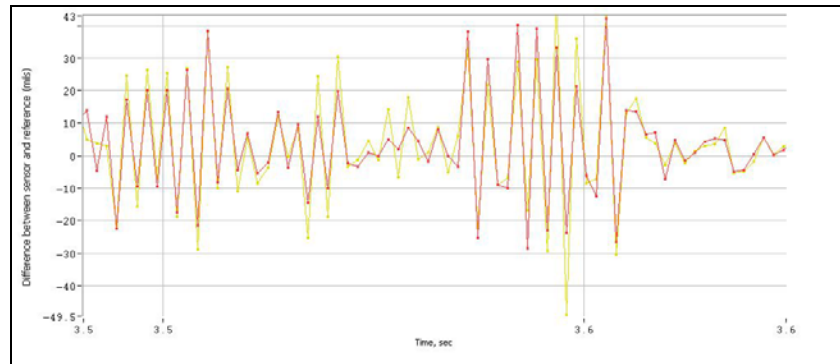


Figure 20. Expanded raw timing data

From the above plot, much information can be gathered. As previously stated, this data corresponded to light probes three and four, which were mounted at 267.3° and 250.9° respectively, with probe three near the leading edge and probe four at the half chord. Since the probes were very closely spaced together in the casing and mounted at different axial locations on the blade, the above plot shows that the blades were responding in the first bending mode. This can be seen because the amplitude of displacement for both probes relative to the anticipated position was nearly the same, at exactly the same time. This shows that transverse displacement was independent of chord position, which signifies a bending mode. A torsion mode would have leading and trailing edge of the blades being maximum values.

D. EXPERIMENTAL CAMPBELL DIAGRAM DEVELOPMENT

A fast Fourier transform (fft) was done on the relevant RPM data. No smoothing function was applied to the data and the timing data was referenced to the rotor mean. The applied fft was 512 points, with one average and 50% bin overlap. The fft looked at the frequency spectrum through the surge cycle with time on the ordinate, and engine order on the abscissa. The fft of the raw data yielded the following waterfall plot. Each frequency band seen below corresponded to a specific stall event in the surge cycle.

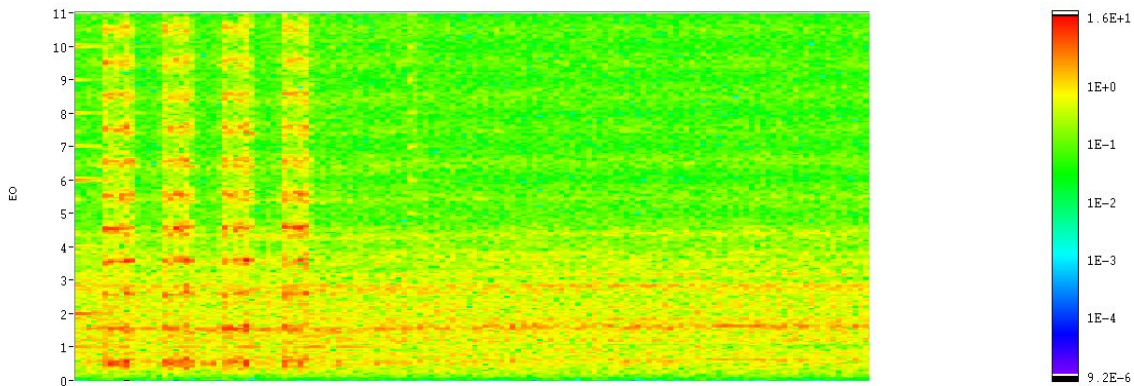


Figure 21. Waterfall plot

From this waterfall plot multiple areas of interest were chosen that corresponded to the maximum displacement (those frequencies) at lower engine orders were analyzed. The software used the data from the specified location on the plot to guess the best nodal diameter (N) of the blade.

The concept of a nodal diameter can be best described as similar to a type of vibrating membrane, where there exists a section of blades having positive displacement and a section where all blades have negative displacement. For example, an N=0 nodal diameter at first bending mode means that the transverse motion of all blades move at first bending and are in phase with each other. N=1 means that 2 blades on opposite sides of the compressor will be 180 degrees out of phase. At N=2 first bending, all blades separated by 90 degrees will be 180 degrees out of phase.

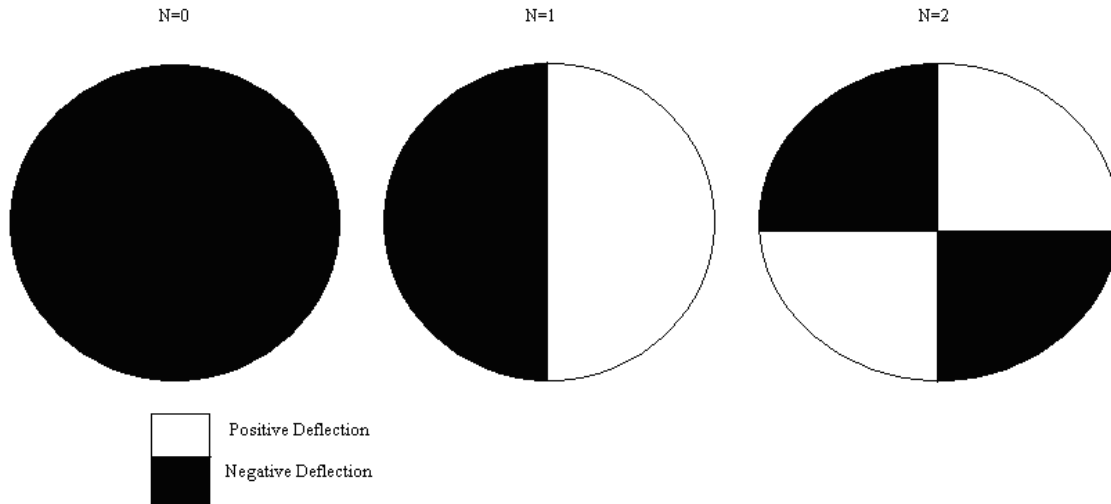


Figure 22. Nodal diameter description

Once the best nodal diameter had been fit to the data, the true frequency of the data was calculated. The true frequency was used on the experimental Campbell diagram. The following equation was used to develop that true frequency:

Equation 1: True Frequency Calculation

$$\omega_{observed} = \omega_{true} + N\omega_{shaft}$$

where the observed frequency is the frequency calculated from the timing data. The calculated true frequency was plotted with respect to engine speed and formed the experimental Campbell diagram shown below.

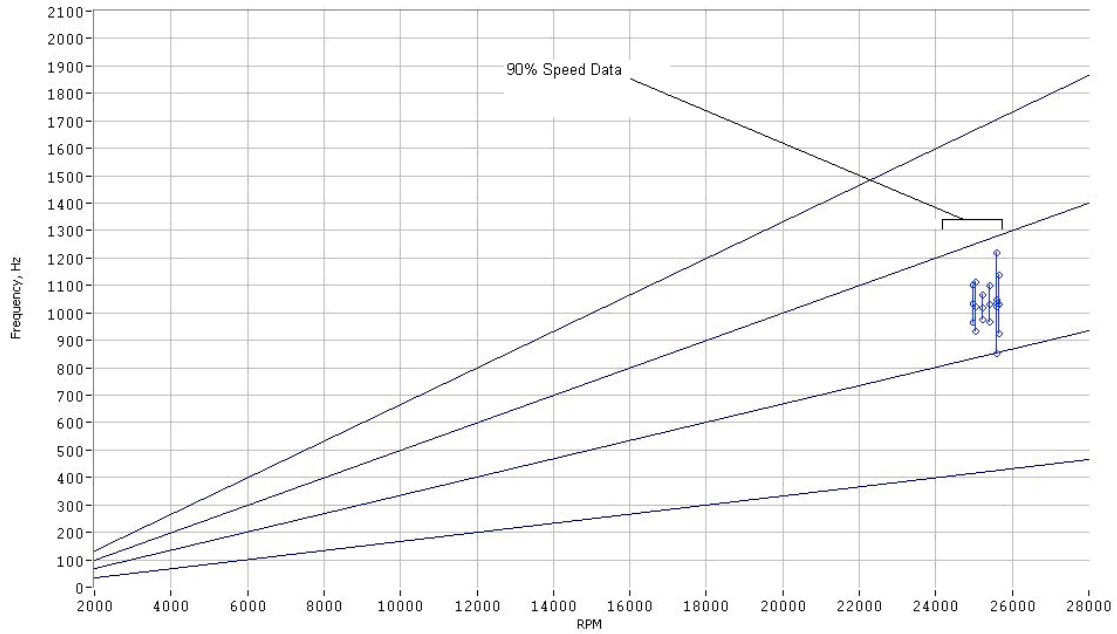


Figure 23. Campbell diagram single data set

The same process for all test speeds was conducted to generate true frequency data across the tested speed spectrum. The data was generated for 80, 90, and 95 percent speed. The Campbell diagram below shows this data.

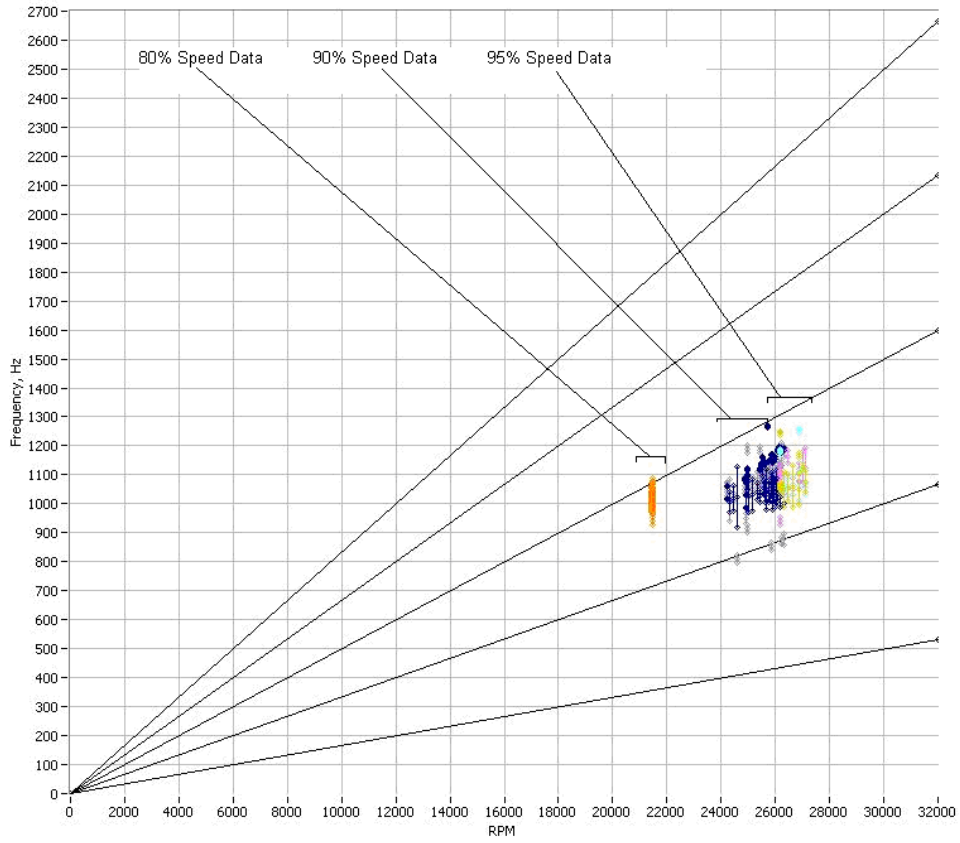


Figure 24. Campbell diagram all data

E. THEORETICAL TO EXPERIMENTAL COMPARISON

In comparison to the theoretical Campbell diagram, the experimental data proved very similar. The overlaid NASA predictions are reproduced on the experimental data in Figure 25.

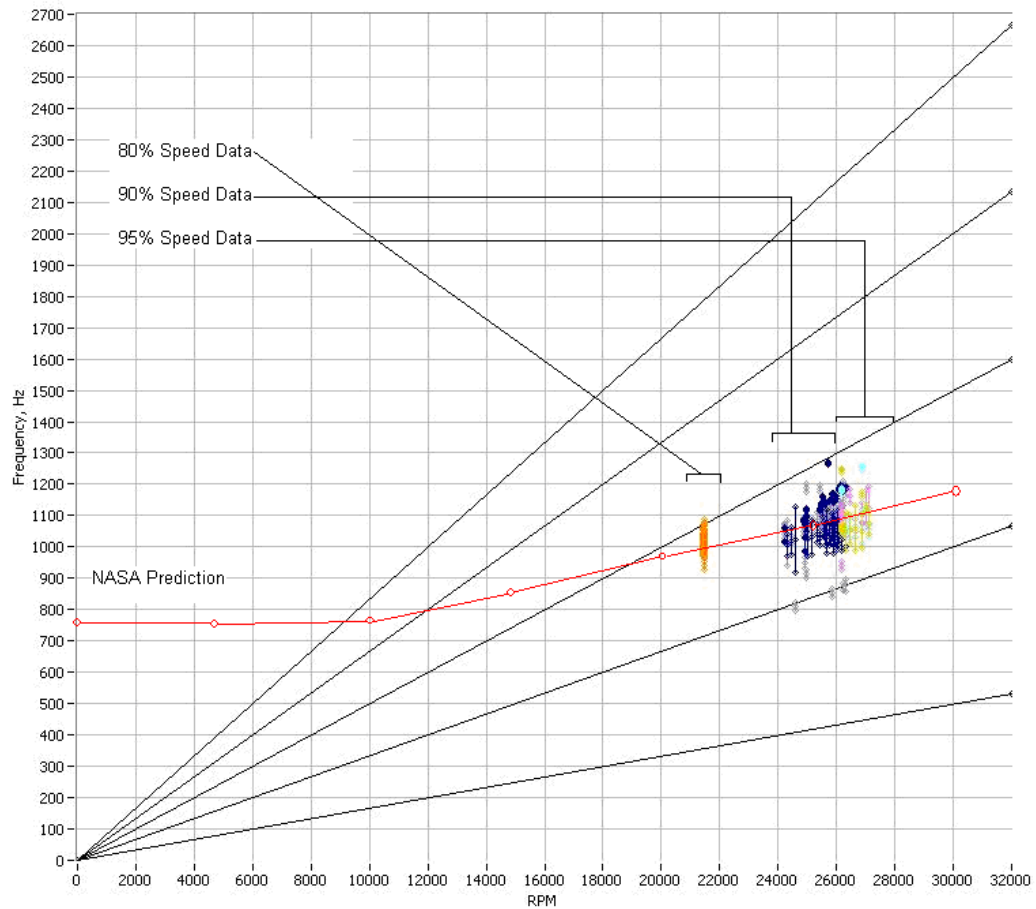


Figure 25. Campbell diagram side by side comparison

From this comparison it can be seen that the average of the data sets at each speed test match closely to theoretical first bending prediction.

Table 5. Campbell diagram comparison

	Measured Natural Frequency (Hz)		Experimental Frequency(Hz) (Excluding Outliers)		
		Color	Nodal Diameter	Maximum	Minimum
80% Speed	990	Orange	-1	1090	975
90% speed	1010	Blue	7	1150	950
		Purple	-1	1150	1010
95% speed	1050	Pink	-1	1190	1050
		Green	7	1189	1050

THIS PAGE INTENTIONALLY LEFT BLANK

V. CONCLUSIONS AND RECOMMENDATIONS

Laser light probes were successfully installed on the NPS transonic compressor and used to determine blade vibration modes at varying speeds. The slope of the theoretical Campbell diagram provided by NASA closely matched the experimental results of the Sanger compressor blade. Higher rotor speed leads to untwisting of the blades which can be seen in the increasing frequency of the first bending mode of the blade data. It was shown that the primary mode observed in the experimentation was the first bending mode. Furthermore, it was seen that during the stall event at maximum deflection the displacement of the blade relative to the expected position was on the order of 30 mils, a significant increase over any other recorded deflection throughout the engine cycle. From the data, operational areas of avoidance were developed. Certain engine speeds and throttle settings were shown to correspond to the greatest blade deflections.

The most important aspect for further research is the examination of lower engine speed tests. Since first bending mode was the primary mode excited, it is imperative to look at its predicted interactions between moderately high engine orders which means lower engine speeds. Specifically, the intersection between the first bending mode and the third engine order, occurring at approximately 70% engine speed would be beneficial to examine. If that engine speed is high enough to excite the first bending mode at the third engine order, the blades would be placed under tremendous intermittent loading. This could result in rapid structural blade fatigue. Quick acceleration through this engine speed could prove advantageous to prolonging blade life. Since this experiment only tested 80 through 95 percent engine speed, no direct conclusion can be made about that specific interaction.

Furthermore, the implementation of multiple sensors mounted along the blade chord could be used to observe torsion modes of the system. A more accurate engine RPM monitoring system could be employed to record a better RPM trace, increasing the fidelity of all aspects of the data.

THIS PAGE INTENTIONALLY LEFT BLANK

LIST OF REFERENCES

- 1] L. E. Kinsler, A. R. Frey, A. B. Coppens, J.V. Sanders, Fundamentals of Acoustics Fourth Edition. New York: John Wiley & Sons, 2000.
- 2] N. G. Osborn, Implementation of a Two-Probe Tip-Timing Technique to Determine Compressor Blade Vibrations. M.S. thesis, Naval Postgraduate School, Monterey, 2000.
- 3] A. J. Sanders, D. C. Rabe, K. K. Hassen, “Experimental and Numerical Study of Stall Flutter in a Transonic Low-Aspect Ratio Fan Blisk” Proceedings of ASME Turbo Expo 2003: Power for Land, Sea, and Air. June 16-19, 2003, Atlanta, Georgia, USA. GT2003-38353.
- 4] P. Tappert, and M. Mercadal, Acquire 8.2 User Manuel. Mt. Hood: Hood Technology Corp, 2007.
- 5] P. Tappert, D. Losh, and M. Mercadal, Analyze Blade Vibration 6.0 User Manual. Mt. Hood: Hood Technology Corp, 2007.
- 6] E. A. Avallone, T. Baumeister, Marks’ Standard Handbook For Mechanical Engineering (tenth edition). New York: McGraw Hill, 1996.
- 7] S. Zarro, Steady-State and Transient Measurements Within a Compressor Rotor During Steam Induced Stall At Transonic Operational Speeds. M.S. thesis, Naval Postgraduate School, Monterey, 2006.
- 8] N. L. Sanger, Design Methodology for the NPS Transonic Compressor p. 58. TPL Technical Note 99-01, August 1999.

THIS PAGE INTENTIONALLY LEFT BLANK

APPENDIX: SOFTWARE INSTRUCTIONS

The Hood Technology Corporation software is in two parts, Acquire Blade Vibration Data 8.2, and Analyze Blade Vibration 6.1 (Analyze 6.0 will not work with two BVS1 boards).

With a properly instrumented system, with probes oriented at varying chord locations and unequally spaced intervals along the casing, data acquisition is very easy.

First open the program, Acquire Blade Data 8.2.

In the top left corner, scroll down to the Acquire mode.

In the PXI/PCI-6602 setup window that opens, enter the clock frequency (either 20 MHz or 80 MHz). The 80MHz clock can cause some problems with two boards due to the programs inability to exactly synchronize the times for each board. The specific probes must be then defined in type and in space. Each board must have a 1/rev reference (use BVM channels 0 and 3). The other channels can be designated for specific probes. The pulse train type for an active probe should read TOA Only. For the channels designated 1/rev the blade number should be 1, otherwise it should correspond to the number of blades in the system. The diameter should be the tip to tip diameter. The location should be the probe location in degrees to a specific reference (if you analyze with time of flight, only the difference is important.) The following setup was used.

BVM Channel	Device	Label	Pulse Train Type	# Blades	Diameter (in)	Location (deg)
0	0	1/rev	TOA Only	1	11	0
1	0	Probe # 4	TOA Only	22	11	250.9
2	0	Probe # 3	TOA Only	22	11	267.3
3	1	1/rev	TOA Only	1	11	0
4	1	Probe # 2	TOA Only	22	11	10.9

Next, the location where the acquired data will be saved can be entered after selecting the "DAQ" tab at the top left of the screen (below acquire selection). The status tab (beside the "DAQ" tab) should be green at all times while taking data. If it turns yellow or red, either the trigger level on the corresponding board should be adjusted, the blade should be cleaned (with a blast of air through the probe hole), or the sensor should be moved closer to the blade. The "RPM" tab traces the RPM of the system.

Once the probes are receiving good data, the “record” button at the top of the screen can be clicked. After the test period, press the “stop” button.

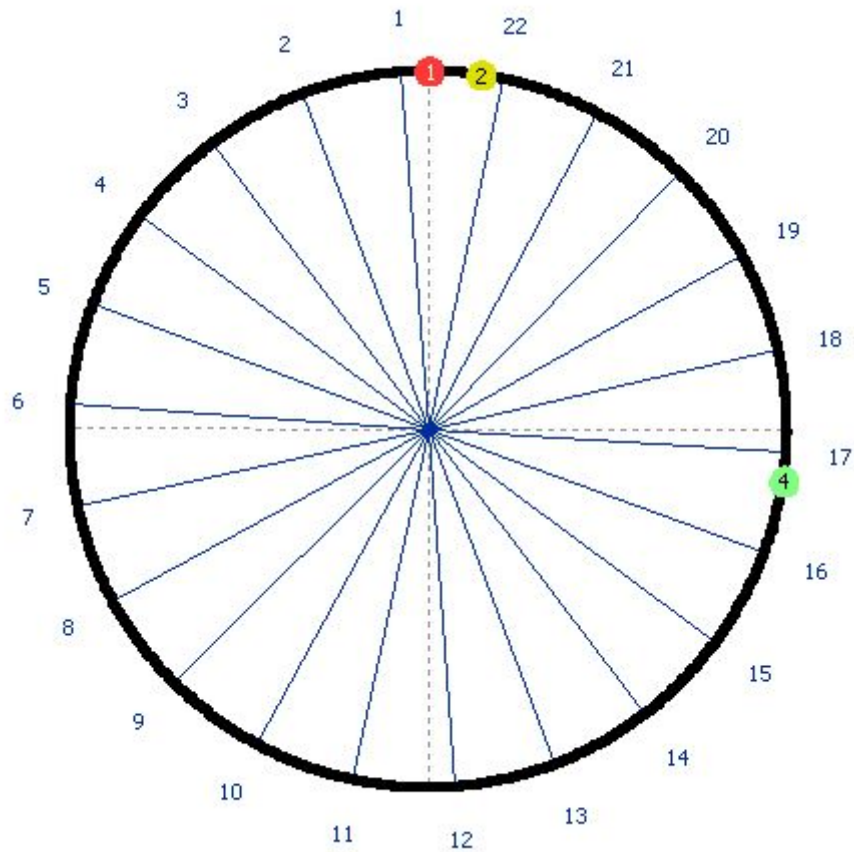
To replay the data, shift the mode from acquire to replay, and select the file you wish to see from the window that opens. The quality of the data can be observed by replaying it. If a probe is intermittent throughout the data, retake that data set.

After the data is observed, it must be analyzed.

To analyze the data, open Analyze Blade Vibration 6.1 (Do not use 6.0 if working with two BVS1 boards).

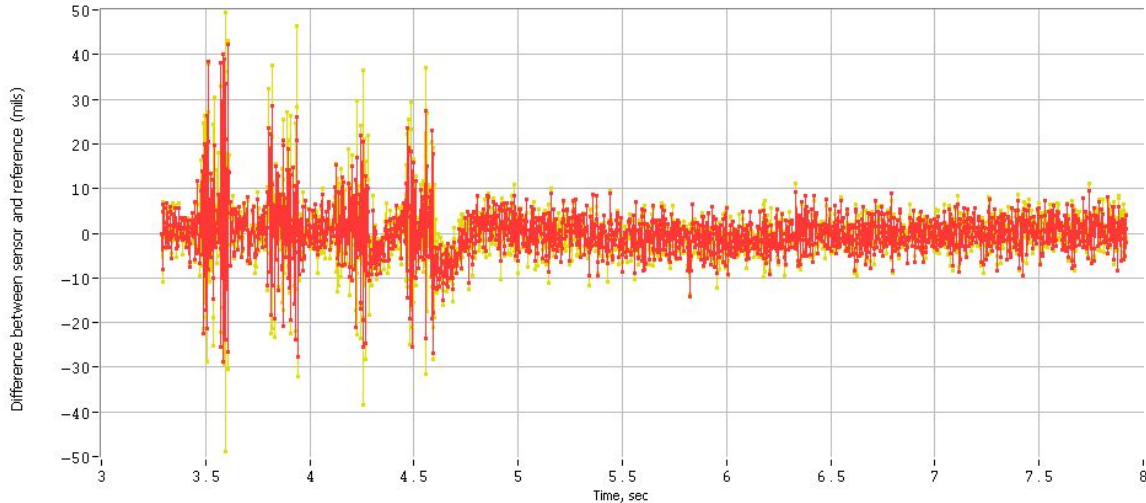
Click on the “select run” tab to determine a data set to be analyzed. Once a data set is chosen, the RPM trace will appear on the screen. The data must then be sorted. Click the “Process Binary” tab and create a new file for the sorted data in the window that appears (name it sorted data for simplicity). Select the new file and click the “current folder” tab at the bottom right of the directory window. Once the data has loaded, press the “OK” tab.

A diagram will then appear on the screen showing a theoretical image of the compressor. Make sure the probe orientation relative to the direction of rotation is correct (remember for a time of flight only the angular difference between sensors being analyzed is important).



To determine the mode of vibration (can only determine first bending mode this way), click on the “Synchronous” tab at the top left of the screen.

At the top of the screen that appears, select the “SDOF curve fit” tab. Below the top figure, change the RPM scale to “time, sec” (by clicking the down arrow). Next, below the top figure, select the sensors to be viewed and their reference. At the right of the screen, change the smoothing parameters to “No Smoothing”, “Ref to Rotor Mean”, and “Do Not Eliminate Outliers.” Finally, at the bottom of the screen, surround the area of interest in the RPM data with the black bars located in the RPM plot (they can be dragged). It should yield a figure of the form:

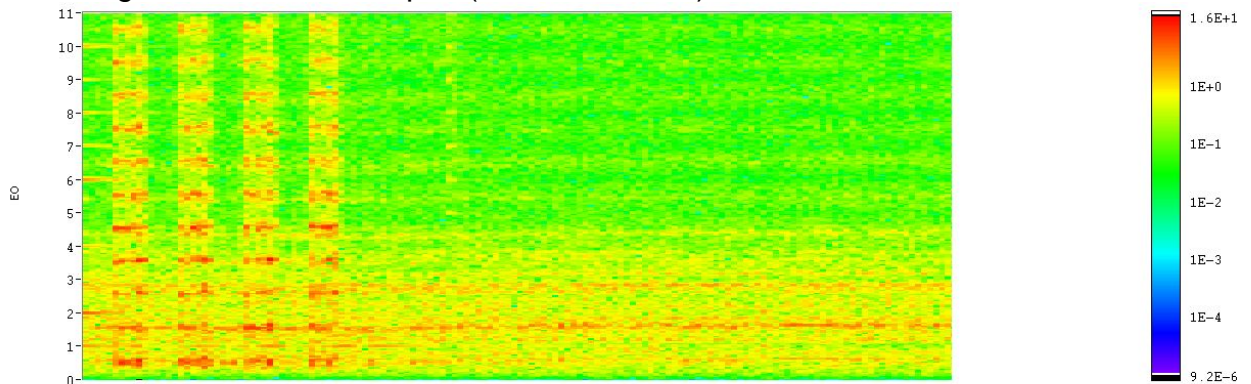


This figure can then be zoomed in on by clicking the magnifying glass to the right of the figure. A box zoom can be completed by choosing the top left option once the magnifying glass has been selected.

If two probes located closely in angular separation on the casing at different point on the chord of the blade have very similar deflections, it can be assumed that a bending mode is being excited.

To analyze the data further, the “Non-Integral” tab at the top of the screen must be selected. For smooth data, change the Npoints in FFT, # Avgs , and % Overlap in the blue box to 512, 1, and 50 respectively. This will result in smoother data. Also in the blue box, the rotor mean must be referenced. Again, surround the interesting point of the RPM trace with the black cursors. Also, click the unlocked button beside both Amplitude (mils) designators underneath the first figure.

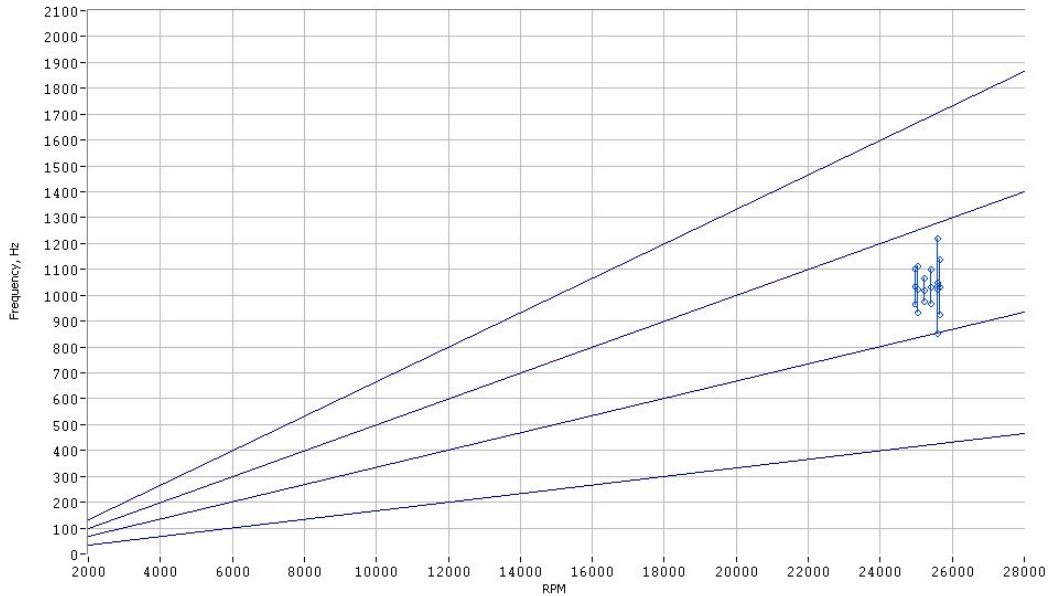
This will generate a waterfall plot (FFT of the data) of the form:



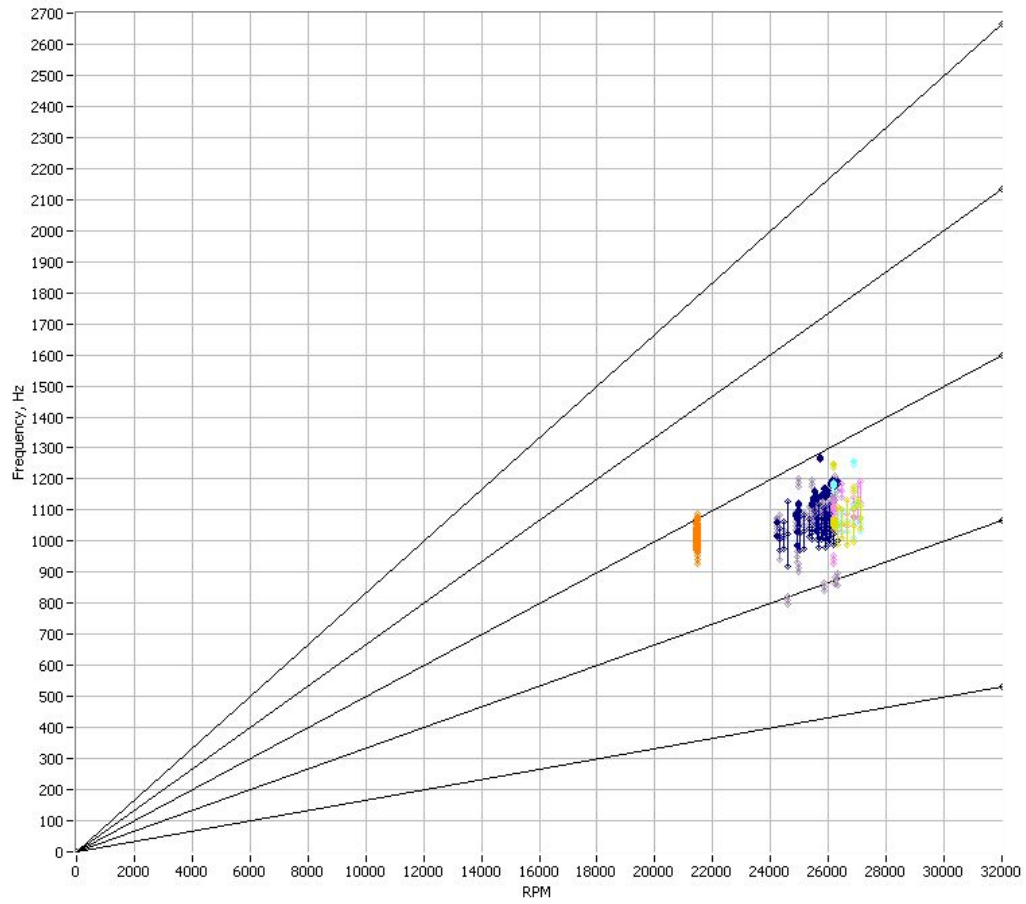
Once the waterfall plot has been generated, surround the area of interest in the waterfall plot with the four black bars on the plot (they can be dragged). Once this is complete click the “Process Nodal Diameter” tab on the screen that arises and

deselect all probes except the Cross:Probe X ref Y (where X and Y are probes of interest). At the bottom right, examine the nodal diameter figure and choose its maximum as the nodal diameter.

Click the “Campbell diagram” tab and change the “Best fit Nodal Diameter” to “Force Nodal Diameter” and insert the maximum from the previous page. The figure should be of the form:



This data can then be overlaid with other run data to form a more comprehensive Campbell Diagram:



INITIAL DISTRIBUTION LIST

1. Defense Technical Information Center
Ft. Belvoir, Virginia
2. Dudley Knox Library
Naval Postgraduate School
Monterey, California
3. Distinguished Professor and Chairmen Anthony Healy
Department of Mechanical and Aeronautical Engineering
Monterey, California
4. Professor Raymond Shreeve
Department of Mechanical and Aeronautical Engineering
Monterey, California
5. Professor Garth Hobson
Department of Mechanical and Aeronautical Engineering
Monterey, California
6. Dr. Anthony Gannon
Department of Mechanical and Aeronautical Engineering
Monterey, California
7. ENS William Murphy
Monterey California